Supporting Information

Interface engineering of RGO/MoS_2/Pd 2D hetrostructure for electrocatalytic overall water splitting in alkaline medium

Ayushi Pandey[1†], Ayan Mukherjee[1†], Sankalpita Chakrabarty[1†], Debabrata Chanda[1] and Suddhasatwa Basu[1,2*]

[1]Department of Chemical Engineering, Indian Institute of Technology Delhi, New Delhi 110016, India

[2] CSIR-Institute of Minerals and Materials Technology Bhubaneswar India

† These authors contributed equally

*Corresponding author, Email: sbasu@iitd.ac.in

1 Experimental section

1.1 Material Synthesis:

1.1.1 Material:

All the precursors were obtained from Sigma Aldrich and used without further purification.

1.1.2 Synthesis:

For the synthesis of MoS_2, 0.23 gm of $(NH_4)_6MO_7O_{24}.4H_2O$ (ammonium molybdate tetrahydrate) and 0.3 gm of CH_3CSNH_2 (thioacetamide) were dispersed in 30 ml of de-ionized (DI) water and kept at stirring for 2h to form exfoliated dispersion followed by addition of 1M NaOH to the solution. In order to maintain the neutral pH of the solution, 1 ml of glacial acetic acid was further added and stirred for another 30 min. The prepared transparent solution was transferred to teflon lined autoclave and kept at 180°C, for 24 h. The final product was collected by centrifugation and washed with DI water and dried overnight to obtain the powder sample. The obtained powder sample was calcined at 100°C for 1 h under N_2 atmosphere to obtain the desired MoS_2.

For the synthesis of RGO-MoS_2 ($RMoS_2$), graphene oxide was prepared by modified hummer's method. 30 mg of as prepared graphene oxide was taken in 30 ml of water and sonicated for 12 h to allow the homogeneous exfoliation of graphene oxide, which is subsequently added to 0.23 g of Ammonium molybdate tetrahydrate and 0.30 g of thioacetamide and followed by the above said steps to obtain the desired $RMoS_2$.

MoS_2Pd was prepared by dispersing 40 mg of as prepared MoS_2 powder in 20 ml of deionized water. The solution was stirred for 8 h and then 10 mg of $PdCl_2$ was added to it, which was stirred for 1 h followed by addition of 10 ml of 50 mM $NaBH_4$ solution and

stirred for another 30 min. The precipitate was collected by centrifugation, washed with DI water and dried at ambient temperature to obtain MoS_2Pd powder.

To prepare $RMoS_2Pd$, 40 mg of $RMoS_2$ powder (prepared as before) was added to 40 ml of deionized water and stirred vigorously for 8 h to obtain well dispersed solution. 10 mg of $PdCl_2$ was added to the solution and stirred for 1 h followed by addition of 10 ml of 50 mM $NaBH_4$ solution and further stirred for 30. The final solution was centrifuged, washed and dried at ambient temperature to obtain $RMoS_2Pd$ powder.

1.2 Characterization:

The X-ray diffraction (XRD) study was carried by Rigaku Miniflex 600 X-ray diffractometer using Cu Kα (λ=1.5418 Å) radiation. Raman analysis is done on Invia Raman microscope under excitation by 514 nm argon ion laser pulse. X-ray photoelectron spectroscopy (XPS) measurement was conducted by Thermo VG scientific Theta Probe instrument with Al Kα target, 1486.6eV energy and maximum power of 15 kW. The transmission electron microscopy (TEM) images were obtained from FEI-Technai-G20 instrument operating at an accelerating voltage of 200 kV. The elemental mapping was characterized by scanning electron microscope (JEOL SEM JSM 6010 LA). Prior to TEM analysis, the aqueous solution of a small amount of sample was dispersed homogeneously in an ultrasonic bath to ensure maximum dispersion of the 2D nanostructure. 2 µl of the solution was cast on a 300 mesh Cu grid, coated with a lacy carbon film and dried at ambient temperature overnight. The Brunauer, Emmett and Teller (BET) analysis was done from N_2 adsorption/desorption isotherm using a Quantachrome Autosorb 1-C instrument. An inductively coupled plasma-mass spectrometry (ICPMS) (Agilent Technologies, 7500 CE, USA) was used to determine the contents of Mo and Pd in the prepared catalysts. The content of C and S was determined from a CHNS analyser (Elementar Vario Macro Cube).

1.3 Electrochemical measurements:

The linear sweep voltammetry (LSV), Chronoamperometry (CA) and electrochemical impedance spectroscopy (EIS) were recorded by using a potentiostat-galvanostat (Autolab, PGSTAT 30, GPES) in the conventional three-electrode assembly at ambient temperature. A glassy carbon (GC) electrode of 3 mm diameter, a platinum wire and Ag/AgCl saturated in KCl was used as the working electrode, counter electrode and reference electrode, respectively. In order to prepare the homogeneous catalyst slurry, 1 mg of electrocatalysts was dispersed in desired amount of Nafion (5 wt. %)/ethanol solution and ultrasonicated for 30 min, which was deposited on the tip of a GC electrode and dried at ambient conditions. The final catalyst loading was 0.35 $mg.cm^{-2}$. The electrolyte used throughout the electrochemical measurements was freshly prepared 1 M KOH solution for all the catalysts. The potentials were measured against Ag/AgCl (saturated KCl) and then converted to RHE. The EIS was recorded in the frequency range of 0.1 Hz to 1 MHz at an applied voltage of 100 mV. All the electrochemical data presented in the manuscript are iR corrected and the polarisation curves are measured at scan rate of 10 $mV.s^{-1}$.

2. Result and discussions

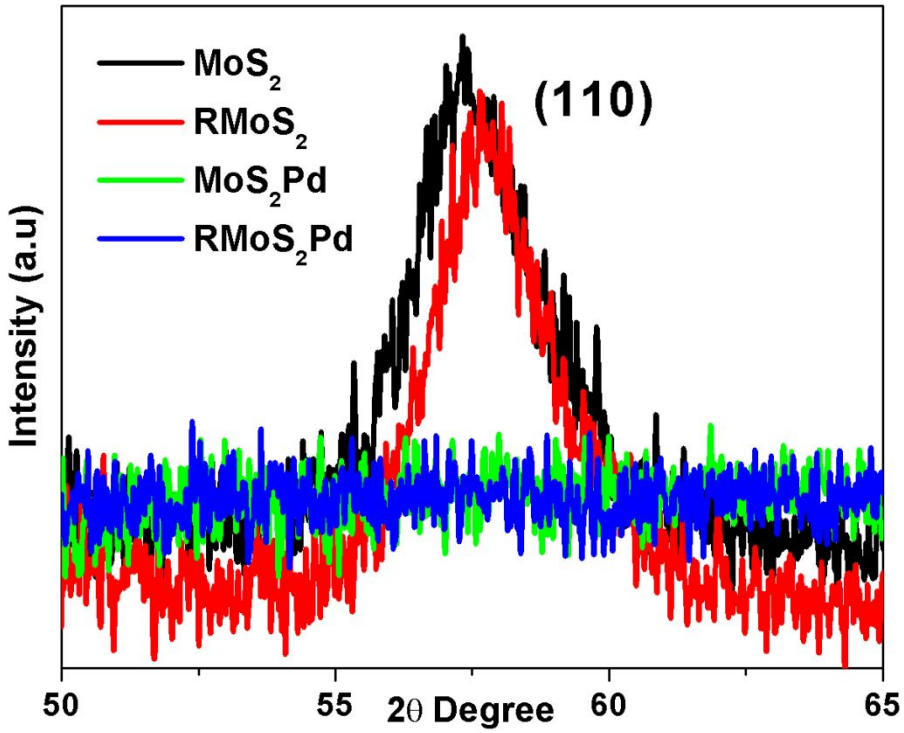

Fig. S1 XRD pattern of all the catalysts at 2Θ = 50º to 65º

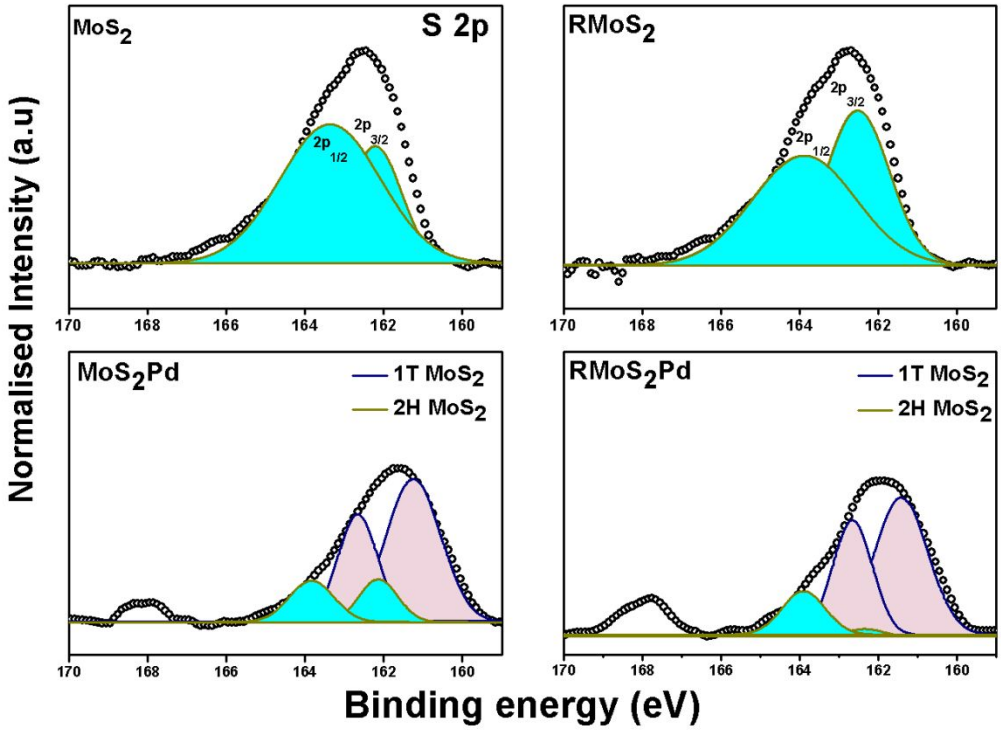

Fig. S2 Normalised S2P spectra by Mo 3d intensity for MoS_2, $RMoS_2$, MoS_2Pd and $RMoS_2Pd$

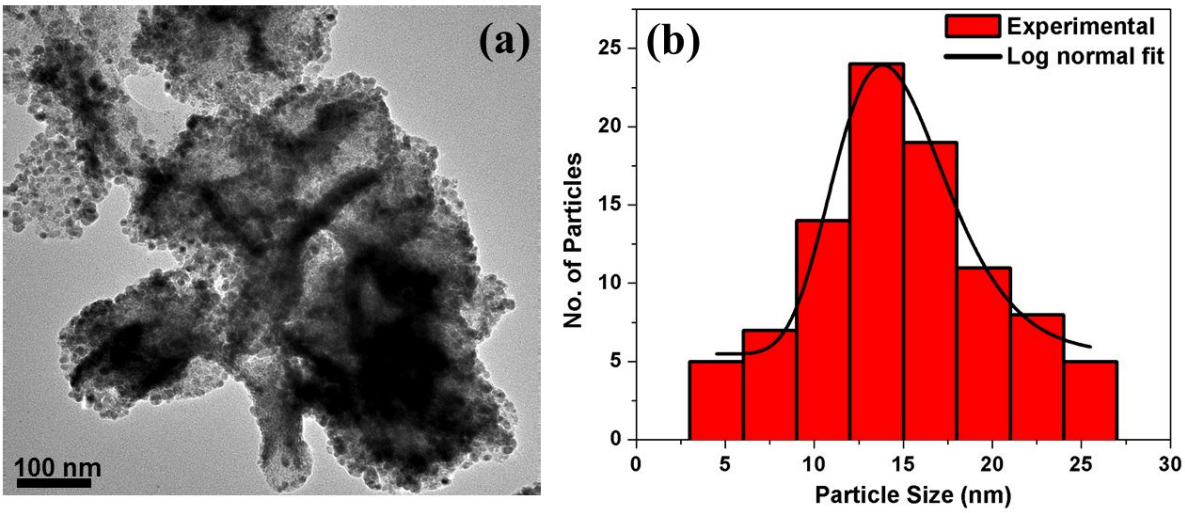

Fig. S3 (a) Representative TEM image of $RMoS_2Pd$, (b) corresponding log normal fitting taken from (a)

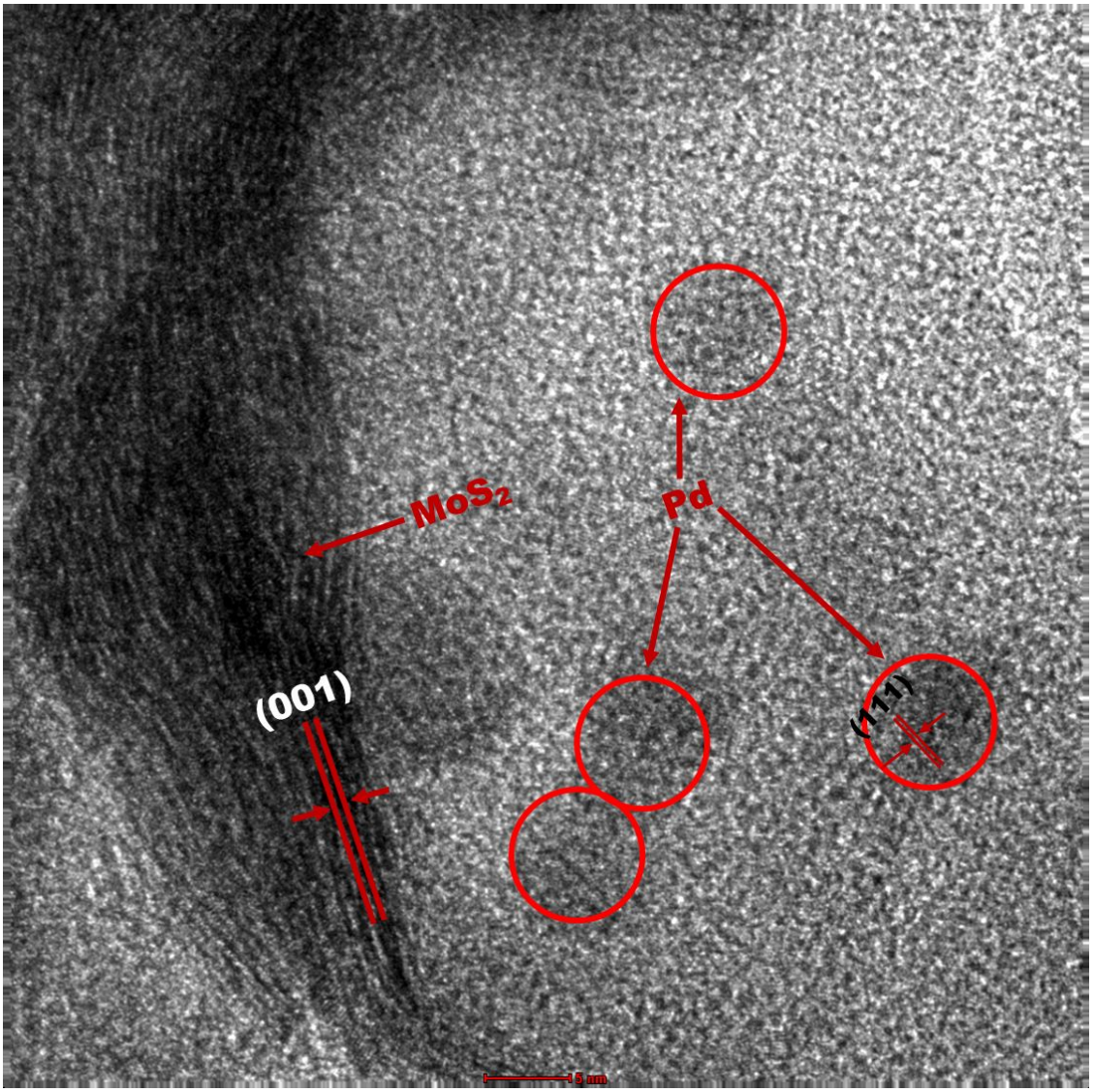

Fig. S4 HRTEM image of $RMoS_2Pd$

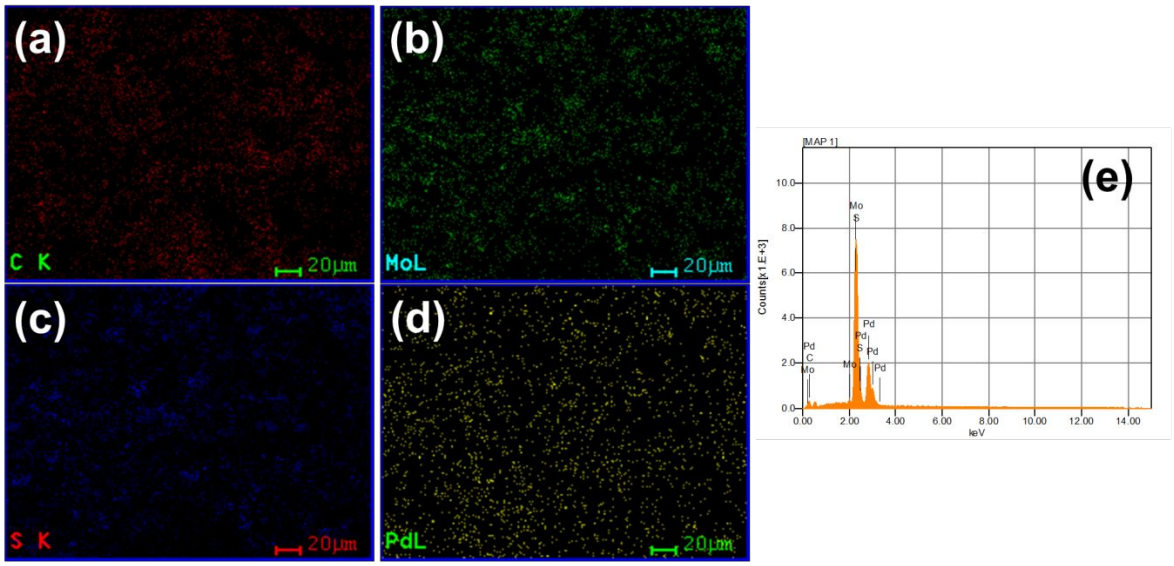

Fig. S5. EDS-mapping of $RMoS_2Pd$ (a) carbon, (b) Mo, (c) S, (d) Pd and (e) EDS spectra

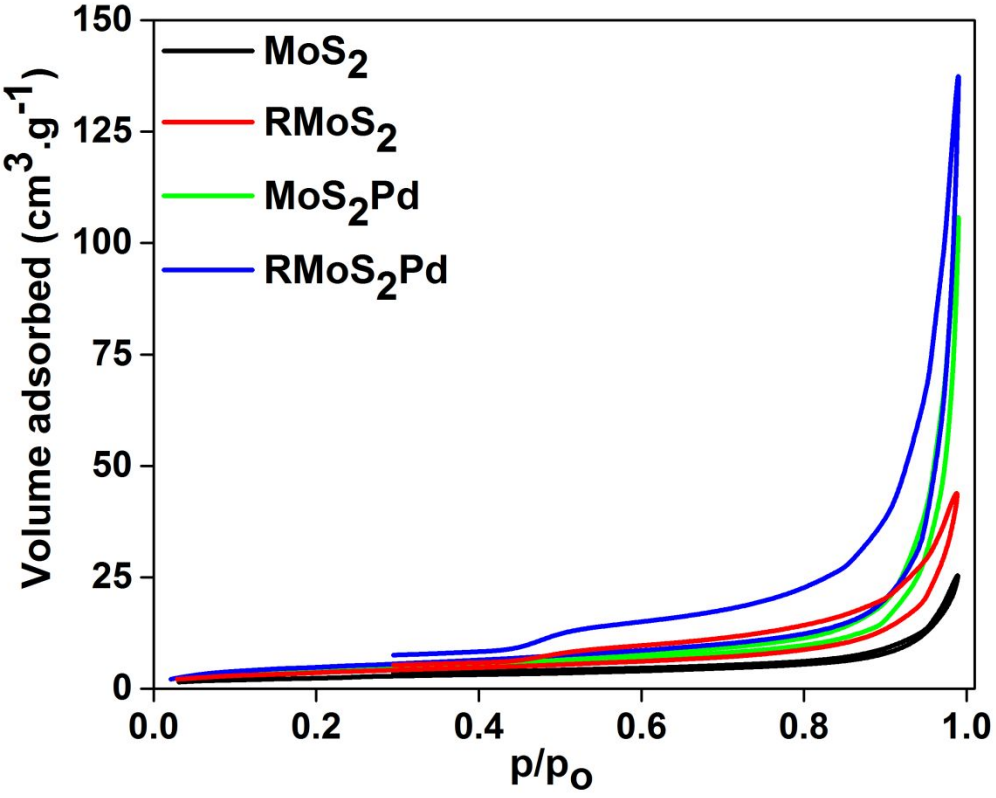

Fig. S6 N_2 adsorption/desorption spectra of all the catalysts

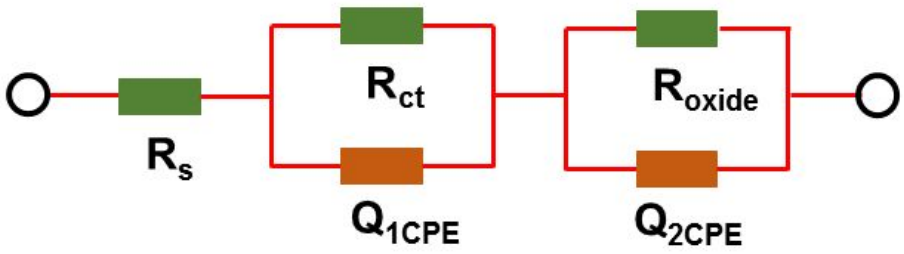

Fig. S7 Equivalent circuit model from Nyquist plot

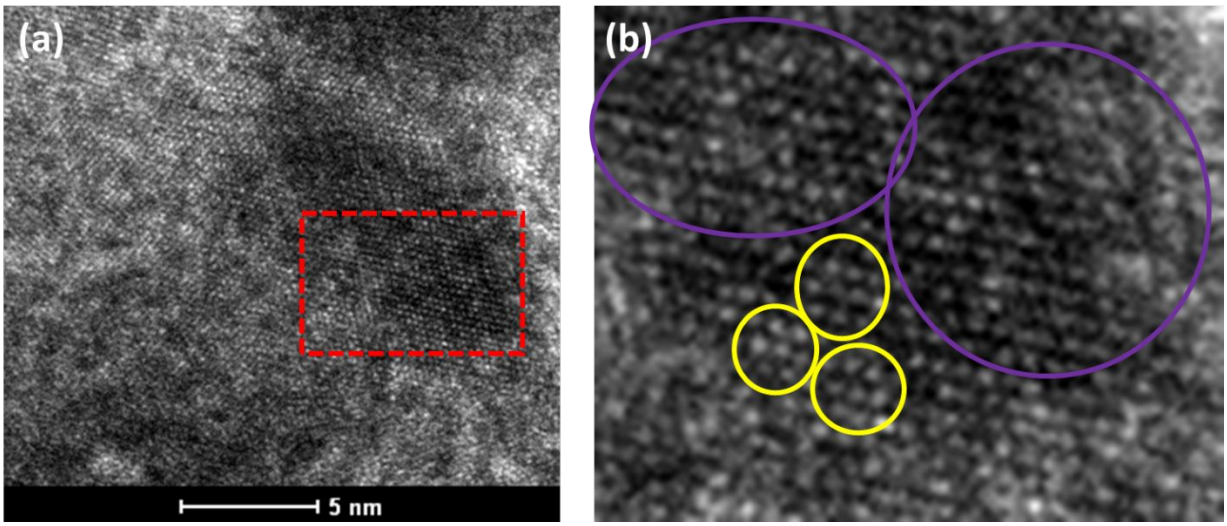

Fig. S8 (a) Post mortem HRTEM image of $RMoS_2Pd$ after OER, (b) magnified view of the portion marked in red in (a)

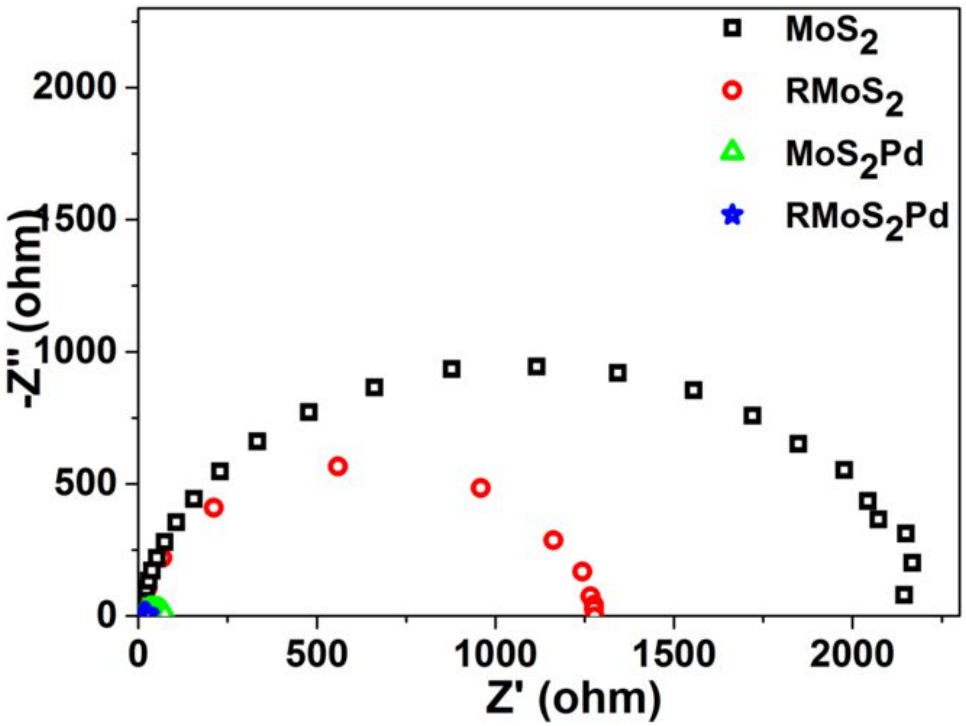

Fig. S9 Nyquist plot for all catalyst in HER

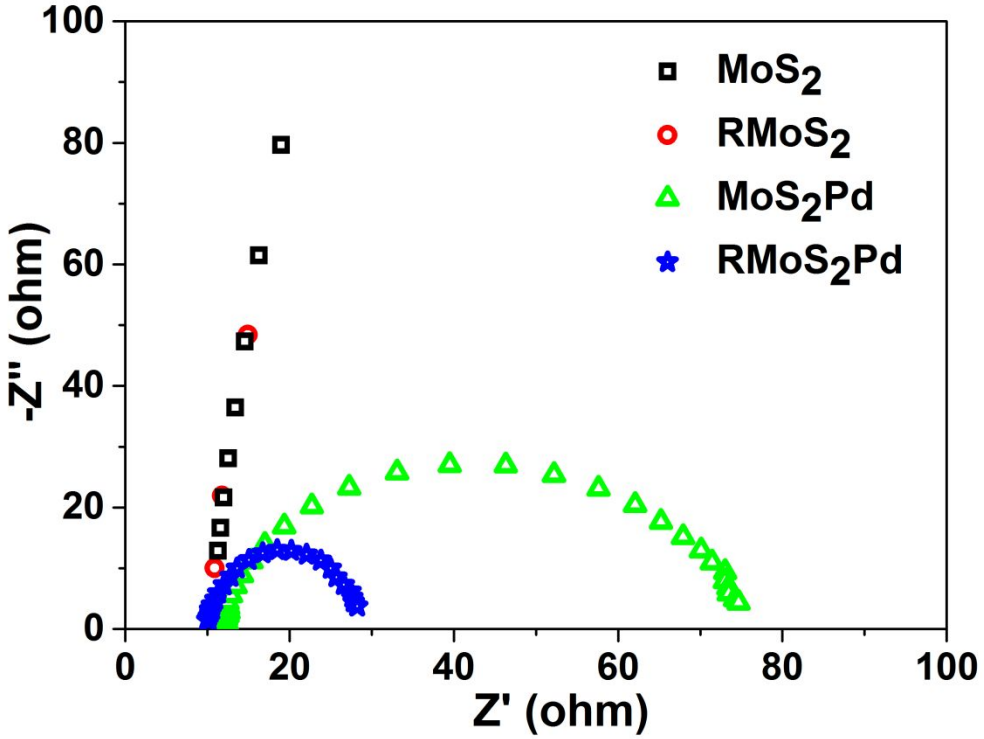

Fig. S10 Magnified view of Fig. S9

Table S1 Average of three measurement results of ICPMS and CHNS analysis for all catalysts

Catalysts	ICPMS (µg.mg^{-1})		%	
	Mo	Pd	C	S
MoS_2	103.01	0.00	0.00	22.81
$RMoS_2$	99.74	0.00	6.95	22.43
MoS_2Pd	98.97	8.56	0.00	16.23
$RMoS_2Pd$	97.46	7.87	7.23	15.40

Table S2 Performance of various catalysts towards OER and HER

Catalyst	OER		HER		Electrolyte	Reference
	Overpotential @10 mA.cm^{-2} (mV vs RHE)	Tafel slope (mV.dec^{-1})	Overpotential @10 mA.cm^{-2} (mV vs RHE)	Tafel slope (mV.dec^{-1})		
$RMoS_2Pd$	245	42	86	35.9	1 M KOH	This work
MoS_2Pd	330	68	114	45.4	1 M KOH	This work
Co_2P/Co foil	319	79	157	59	1 M KOH	[1]
Co_4Mo_2@NC	330	48.7	218	73.5	1 M KOH	[2]
Ni_2P	290	59	220	---	1 M KOH	[3]
Ni_2P-RGO	260	62	142	58	1 M KOH	[4]
lepidocrocite VOOH	270	68	164	104	1 M KOH	[5]
$SrNb_{0.1}Co_{0.7}Fe_{0.2}O_{3-\delta}$ perovskite nanorods	390	61	262	134	0.1 M KOH	[6]
MoS_2-Ni_3S_2	249	57	98	61	1 M KOH	[7]
Ni_3FeN/r-GO	270	54	94	90	1 M KOH	[8]
Ni–Fe–P@C NRs	217	40	79	92.6	1 M KOH	[9]
(MOF-derived) CoSx@MoS_2	347*	147*	239**	103**	*1 M KOH **0.5 M H_2SO_4	[10]
Co_3S_4@MoS_2	330*	59*	210**	88**	*1 M KOH **0.5 M H_2SO_4	[11]
Ni–Co–P HNB	270	76	107	46	1 M KOH	[12]
MoS_2/CF-750	---	---	125	34	0.5 M H_2SO_4	[13]
MoS_2@HG	---	----	124	41	0.5 M H_2SO_4	[14]

MnO_2-CoP_3/Ti	288	65	---	---	1 M KOH	[15]
CoS_2@MoS_2/RGO	--	--	98	37.4	0.5 M H_2SO_4	[16]

References

(1) Yuan, C. Z.; Zhong, S. L.; Jiang, Y. F.; Yang, Z. K.; Zhao, Z. W.; Zhao, S. J.; Jiang, N.; Xu, A. W. Direct Growth of Cobalt-Rich Cobalt Phosphide Catalysts on Cobalt Foil: An Efficient and Self-Supported Bifunctional Electrode for Overall Water Splitting in Alkaline Media. *J. Mater. Chem. A* **2017**, *5* (21), 10561–10566.

(2) Jiang, J.; Liu, Q.; Zeng, C.; Ai, L. Cobalt/Molybdenum Carbide@N-Doped Carbon as a Bifunctional Electrocatalyst for Hydrogen and Oxygen Evolution Reactions. *J. Mater. Chem. A* **2017**, *5* (32), 16929–16935.

(3) Stern, L. A.; Feng, L.; Song, F.; Hu, X. Ni2P as a Janus Catalyst for Water Splitting: The Oxygen Evolution Activity of Ni2P Nanoparticles. *Energy Environ. Sci.* **2015**, *8* (8), 2347–2351.

(4) Yan, L.; Jiang, H.; Xing, Y.; Wang, Y.; Liu, D.; Gu, X.; Dai, P.; Li, L.; Zhao, X. Nickel Metal-Organic Framework Implanted on Graphene and Incubated to Be Ultrasmall Nickel Phosphide Nanocrystals Acts as a Highly Efficient Water Splitting Electrocatalyst. *J. Mater. Chem. A* **2018**, *6* (4), 1682–1691.

(5) Shi, H.; Liang, H.; Ming, F.; Wang, Z. Efficient Overall Water-Splitting Electrocatalysis Using Lepidocrocite VOOH Hollow Nanospheres. *Angew. Chemie - Int. Ed.* **2017**, *56* (2), 573–577.

(6) Zhu, Y.; Zhou, W.; Zhong, Y.; Bu, Y.; Chen, X.; Zhong, Q.; Liu, M.; Shao, Z. A Perovskite Nanorod as Bifunctional Electrocatalyst for Overall Water Splitting. *Adv. Energy Mater.* **2017**, *7* (8), 1602122.

(7) Yang, Y.; Zhang, K.; Lin, H.; Li, X.; Chan, H. C.; Yang, L.; Gao, Q. MoS_2–Ni_3S_2 Heteronanorods as Efficient and Stable Bifunctional Electrocatalysts for Overall Water

Splitting. *ACS Catal.* **2017**, *7* (4), 2357–2366.

(8) Gu, Y.; Chen, S.; Ren, J.; Jia, Y. A.; Chen, C.; Komarneni, S.; Yang, D.; Yao, X. Electronic Structure Tuning in Ni3FeN/r-GO Aerogel toward Bifunctional Electrocatalyst for Overall Water Splitting. *ACS Nano* **2018**, *12* (1), 245–253.

(9) Ahn, S. H.; Manthiram, A. Direct Growth of Ternary Ni-Fe-P Porous Nanorods onto Nickel Foam as a Highly Active, Robust Bi-Functional Electrocatalyst for Overall Water Splitting. *J. Mater. Chem. A* **2017**, *5* (6), 2496–2503.

(10) Chakrabarty, S.; Mukherjee, A.; Basu, S. RGO-MoS2Supported NiCo2O4 Catalyst toward Solar Water Splitting and Dye Degradation. *ACS Sustain. Chem. Eng.* **2018**, *6* (4), 5238–5247.

(11) Guo, Y.; Tang, J.; Qian, H.; Wang, Z.; Yamauchi, Y. One-Pot Synthesis of Zeolitic Imidazolate Framework 67-Derived Hollow Co_3S_4@MoS_2 Heterostructures as Efficient Bifunctional Catalysts. *Chem. Mater.* **2017**, *29* (13), 5566–5573.

(12) Hu, E.; Feng, Y.; Nai, J.; Zhao, D.; Hu, Y.; Lou, X. W. Construction of Hierarchical Ni-Co-P Hollow Nanobricks with Oriented Nanosheets for Efficient Overall Water Splitting. *Energy Environ. Sci.* **2018**, *11* (4), 872–880.

(13) Cheng, Y.; Pang, K.; Wu, X.; Zhang, Z.; Xu, X.; Ren, J.; Huang, W.; Song, R. In Situ Hydrothermal Synthesis MoS2/Guar Gum Carbon Nanoflowers as Advanced Electrocatalysts for Electrocatalytic Hydrogen Evolution. *ACS Sustain. Chem. Eng.* **2018**, *6* (7), 8688–8696.

(14) Han, X.; Tong, X.; Liu, X.; Chen, A.; Wen, X.; Yang, N.; Guo, X.-Y. Hydrogen Evolution Reaction on Hybrid Catalysts of Vertical MoS2 Nanosheets and Hydrogenated Graphene. *ACS Catal.* **2018**, acscatal.7b03316.

(15) Xiong, X.; Ji, Y.; Xie, M.; You, C.; Yang, L.; Liu, Z.; Asiri, A. M.; Sun, X. MnO2-CoP3nanowires Array: An Efficient Electrocatalyst for Alkaline Oxygen Evolution Reaction with Enhanced Activity. *Electrochem. commun.* **2018**, *86* (November 2017), 161–165.

(16) Guo, Y.; Gan, L.; Shang, C.; Wang, E.; Wang, J. A Cake-Style CoS2@MoS2/RGO Hybrid Catalyst for Efficient Hydrogen Evolution. *Adv. Funct. Mater.* **2017**, *27* (5), 1–7.